

NUMERICAL MODELING OF RAILWAY TRACK SUPPORTING SYSTEM USING FINITE-INFINITE AND THIN LAYER ELEMENTS

J. Noorzaei, W.A.M. Thanoon, W.F. Yeat
P. Moradi Pour and M.S. Jaafar*

*Department of Civil Engineering, Faculty of Engineering, Universiti Putra Malaysia
43400 UPM Serdang, Selangor Darul Ehsan, Malaysia
jamal@eng.upm.edu.my - walid@eng.upm.edu.my - yeat@eng.upm.edu.my
parviz.mop@gmail.com - msj@eng.upm.edu.my*

*Corresponding Author

(Received: February 14, 2008 – Accepted in Revised Form: September 25, 2008)

Abstract The present contribution deals with the numerical modeling of railway track-supporting systems-using coupled finite-infinite elements-to represent the near and distant field stress distribution, and also employing a thin layer interface element to account for the interfacial behavior between sleepers and ballast. To simulate the relative debonding, slipping and crushing at the contact area between sleepers and ballast, a modified Mohr-Coulomb criterion was adopted. Further more an attempt was made to consider the elasto plastic materials' non-linearity of the railway track supporting media by employing different constitutive models to represent steel, concrete and other supporting materials. It is seen that during an incremental-iterative mode of load application, the yielding initially started from the edge of the sleepers and then flowed vertically downwards and spread towards the center of the railway supporting system.

Keywords Thin Layer Element, Finite Element, Infinite Element, Railway Track Supporting Media

چکیده تحقیق حاضر به مدل سازی عددی سیستم های تکیه گاهی واگن های راه آهن با استفاده از المان های محدود-نامحدود متناهی-نامتناهی جهت نمایش میدان های تنش دور و نزدیک می پردازد. همچنین برای بررسی رفتار بین وجهی، المان نازک فصل مشترک تراورس و خرده سنگ نیز به کار گرفته شده است. برای شبیه سازی گسستگی، لغزش و خوردگی نسبی در محل تماس تراورس و خرده سنگ زیر آن، ضابطه موهر-کولومب اصلاح شده به کار رفت. همچنین سعی شد که مواد ارتجاعی-خمیری و رفتار غیرخطی محیط سیستم تکیه گاهی واگن های راه آهن با به کار بردن مدل های تنش-کرنش مختلف برای فولاد، بتن و مواد تکیه گاهی دیگر در نظر گرفته شود. نتایج نشان می دهد که در مدت تکرار مد اعمال بارگذاری، تسلیم از کناره های تراورس ها شروع و سپس به شکل قائم به سمت پایین و به سمت مرکز سیستم تکیه گاهی راه آهن منتشر می شود.

1. INTRODUCTION

In railway transportation, there is an ongoing demand for increased performance, which is driven by the need to keep a competitive edge against other means of transportation, such as aircrafts, cars and ships. This calls for highly technical requirements in their analysis and design procedures. Most railway track systems consist of rails, sleepers, ballast, sub-ballast and sub-grades. It also is essential to use an analytical model that realistically represents the actual behavior of this

track system when subjected to an actual load. Most investigators made use of finite elements for the purpose of physical and material modeling. For example, a linear elastic analysis was performed for rail track support systems by Desai, et al [1], as well as his earlier work [2] by using three dimensional finite isoparametric brick elements for the aim of discretization.

Chang, et al [3] developed a finite element model, GEOTRACK, to obtain the elastic response of the track substructure. This model considered the three dimensional nature of the soil-track-

ballast, sub-ballast and underling sub-grade soil layer subjected to multi-axle load.

Mauro, et al [4], produced an integrated design methodology, based on the use of a numerical simulation through finite element technique. The results have shown that axle flexibility has an important effect on the wheel-rail forces in a tangent track and so it permits a more accurate calculation of the load spectra, needed for durability analysis. Lombaert, et al [5] proposed a two dimensional model, which accounts for the rail, rail pad, floating slab and the slab mat by ignoring the track soil interface. Michael, et al [6] used the classical model, a beam on an elastic half space to model the slab-track railway system subjected to a vertical axle of a running train.

It is obvious from the literature review that most researchers employed numerically or semi numerical methods to simulate the railway track-sleeper-ballast-sub-ballast-supporting soil. But there is no literature available on the interface modeling between sleeper and ballast. The researchers also ignored the effect of the interaction between the supporting soil and the railway track system. Furthermore no information is available on the nonlinear stress strain relationship of different materials involved in a railway track system and their consequent effect on the behavior of a railway track supporting media.

The aims of the present investigation are:

- (a) To develop a numerical tool using a finite element technique, this is a capable of integrating a railway track supporting media as a single composite unit.
- (b) To couple finite-infinite elements and the interface element for the purpose of idealisation.
- (c) To account for the elasto-plastic constitutive law of the materials involved in a railway track supporting system.

However in the present study the effect of track structure has been neglected.

2. PROPOSED PHYSICAL MODELING OF THE RAILWAY TRACK SUPPORTING SYSTEM

The following elements are used to represent the

railway track supporting system;

- The eight-nodded isoparametric element is used to model the railway track-sleepers and supporting media (Zienkiewicz [7]).
- A five-node infinite element to represent the far field behavior. The coupling of this infinite element with a conversional finite element was presented by Viladkar, et el [8-10]).
- A six node thin layer element to account for the interfacial behavior between the sleepers and the ballast, the detailed formulation of this element are presented in the following article.

Table 1 shows the proposed types of the elements used to model the components of the railway supporting system.

2.1. Finite Element Formulation of the Thin Layer Element

A thin layer element was introduced by Desai, et al [11,12] to simulate the interfacial behavior in a soil-structure interaction structural problem and is adopted in this study. The interface element in this analysis is represented by a six-node thin-layer interface element (Figure 1) with the width of B and thickness t.

The present element is of isoparametric type, hence it can be written as:

$$x = \sum N_i x_i, y = \sum N_i y_i \quad (1)$$

$$u = \sum N_i u_i, v = \sum N_i v_i \quad (2)$$

(i) At the corner

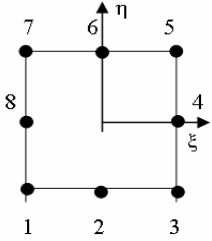
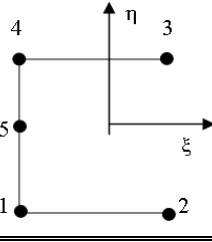
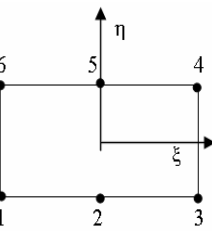
$$N_i = \frac{1}{4} \left(1 + \xi \xi_i \right) \left(1 + \eta \eta_i \right) \left(\xi \xi_i \right) \quad i = 1, 3, 4, 6 \quad (3)$$

(ii) At the mid nodes when $\xi = 0$

$$N_i = \frac{1}{2} \left(1 - \xi^2 \right) \left(1 + \eta \eta_i \right) \quad i = 2, 5 \quad (4)$$

Where u and v are the nodal global displacements in x and direction, N_i is the shape function at the nodes, ξ and η are the local coordinates.

TABLE 1. Two-Dimensional Serendipity Type of Finite, Infinite and Thin Layer Elements.

Types of Element	Element Figure	Shape Functions
Eight-Node Finite Element		For corner nodes (1,3,5,7): $N_i = \frac{1}{4} (1+\xi\xi_i)(1+\eta\eta_i)(\xi\xi_i+\eta\eta_i-1)$ For mid side nodes (2,4,6,8): $N_i = \frac{\xi_i^2(1+\xi\xi_i)(1-\eta^2) + \eta_i^2(1+\eta\eta_i)(1-\xi_i^2)}{2}$
Five-Node Infinite Element		$N_1 = \frac{\xi\eta(1-\eta)}{(1-\xi)} \quad N_4 = \frac{-\xi\eta(1+\eta)}{(1-\xi)}$ $N_2 = \frac{(1+\xi)(-\eta)}{2(1-\xi)} \quad N_5 = \frac{-2\xi(1-\eta^2)}{(1-\xi)}$ $N_3 = \frac{(1+\xi)(1+\eta)}{2(1-\xi)}$
Thin Layer Element		(a) For corner nodes (1,3,4,6): $N_i = \frac{(\xi\xi_i)(1+\xi\xi_i)(1+\eta\eta_i)}{4}$ (b) For mid side nodes (2,5): $N_i = \frac{1}{2} (1-\xi^2)(1+\eta\eta_i)$

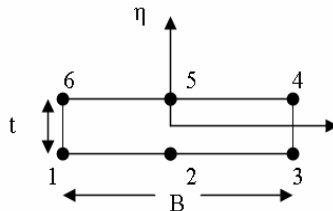


Figure 1. Thin layer interface element.

The normal stress (σ_n) and shear stress (τ) are related to the corresponding normal (ε_n) and tangential (γ) strains in the local coordinate system by:

$$\begin{Bmatrix} \sigma_n \\ \tau \end{Bmatrix} = [\bar{C}_e] \begin{Bmatrix} \varepsilon_n \\ \gamma \end{Bmatrix} \quad (5a)$$

or

$$\{d\sigma\} = [\bar{C}_e] \{d\varepsilon\} \quad (5b)$$

Where

$$\bar{C}_e = \begin{bmatrix} tk_{nn} & 0 \\ 0 & tk_{ss} \end{bmatrix} \quad (6)$$

Where \bar{C}_e is the elastic local constitutive matrix,

k_{nn} and k_{ss} are the normal and shear stiffness, respectively.

The normal (ϵ_n) and shear (γ) strains in the local coordinate system are related to the global strains, ϵ_x , ϵ_y , and γ_{xy} as:

$$\begin{bmatrix} \epsilon_n \\ \gamma \end{bmatrix} = \begin{bmatrix} s^2 & c^2 & -cs \\ -2cs & 2cs & c^2-s^2 \end{bmatrix} \begin{bmatrix} \epsilon_x \\ \epsilon_y \\ \gamma_{xy} \end{bmatrix} \quad (7a)$$

or

$$\{\bar{\epsilon}\} = [T]\{\epsilon\} \quad (7b)$$

Where $s = \sin \theta$, $c = \cos \theta$, $\theta =$ the inclination of the interface to the x-axis and $[T]$ is the transformation matrix of strains from the global vector $\{\epsilon\}$ to the local vector $\{\bar{\epsilon}\}$.

With the use of Equations 5b and 7b, and equating the global and local strain vectors, the following incremental equations can be obtained:

$$\{d\sigma\} = [T]^T [\bar{C}_e] [T] \{d\epsilon\} \quad (8a)$$

$$\{d\sigma\} = [C_e] \{d\epsilon\} \quad (8b)$$

$$[C_e] = \begin{bmatrix} s^2 & -2cs \\ c^2 & 2cs \\ -cs & (c^2-s^2) \end{bmatrix} \begin{bmatrix} tk_{nn} & 0 \\ 0 & tk_{ss} \end{bmatrix} \begin{bmatrix} s^2 & c^2 & -cs \\ -2cs & 2cs & (c^2-s^2) \end{bmatrix} \quad (9)$$

Where $[C_e]$ is the global constitutive matrix and $\{d\sigma\}$ and $\{d\epsilon\}$ are global stress and strain vectors.

When $\theta = 0$ in the transformation matrices the horizontal interface in Equation 9, will be reduced to:

$$[C_e] = \begin{bmatrix} 0 & 0 & 0 \\ 0 & tk_{nn} & 0 \\ 0 & 0 & tk_{ss} \end{bmatrix} \quad (10)$$

Hence the global stiffness matrix of the thin layer

element can be determined as:

$$[K] = \int_v [B]^T [C_e] [B] dv \quad (11)$$

2.2. Elasto-Plastic Constitutive Models To simulate the relative debonding, slipping and crushing that could take place in the contact area between the sleeper and ballast, a modified Mohr-Coulomb criterion was adopted (Linsbauer, et al [13]).

Figure 2 shows the three possible regions for failure i.e. debonding, slipping and crushing failures. Elasto-plastic constitutive laws evolved in different regions based on the theory of plasticity with associated flow rules as shown in Table 2.

In Table 2, σ_n and τ are normal and shear stress respectively, f_t and f_c are tensile and compressive strength respectively, ϕ is the friction angle, γ is $\tan \phi \tan \psi$, ψ is the dilatancy angle and ($\phi = \psi$) when the plastic flow is associated, c is the cohesion.

3. SOLUTION ALGORITHM FOR ELASTO-PLASTIC FE ANALYSIS

The incremental-iterative procedure has been adopted for the nonlinear finite element elasto-plastic analysis of a railway track supporting system. The load is applied in several steps as increments. The load steps can be of equal or unequal increments in nature. The displacement increments are evaluated using the tangent stiffness matrix $[K]$ of the previous load increment that is;

$$[K]_{i-1} \{\Delta\delta\}_i = \{\Delta F\}_i \quad (12)$$

Where $[K]_{i-1}$ is the stiffness matrix of the previous load increment.

$\{\Delta\delta\}_i, \{\Delta F\}_i$ is the current displacement and load vector respectively.

These displacement increments are accumulated to give the total displacement at any stage of loading:

$$\{\Delta\}_i = \{\Delta\}_{i-1} + \{\Delta\delta\}_i \quad (13)$$

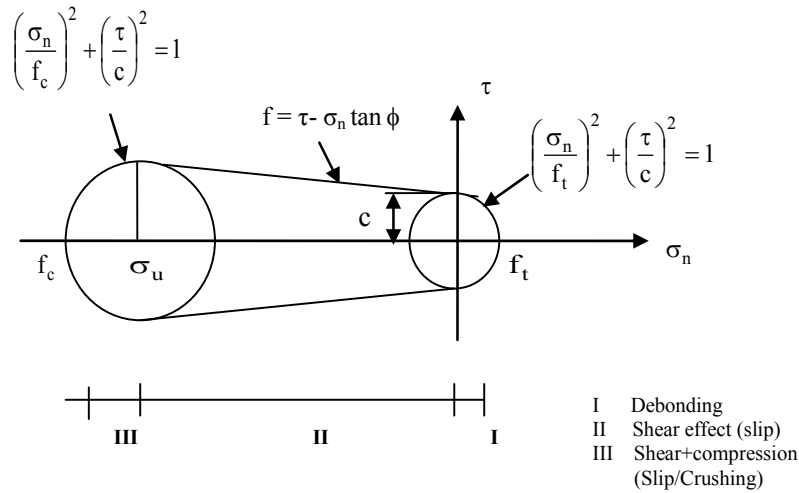


Figure 2. Modified mohr-coulomb criterion (Linsbauer [13]).

TABLE 2. Modes of Deformation of a Thin Layer Interface and Corresponding Constitutive Models.

Modes of Deformation	Elasto-Plastic Matrix	
Debonding	$[D_{ep}] = \frac{t}{k_{ss}\tau_f^2 + k_{nn}\sigma_n^2 c^4}$	$\begin{bmatrix} 0 & 0 & 0 \\ 0 & k_{nn}k_{ss}\tau_f^4 & -k_{nn}k_{ss}\tau\sigma_n c^2 f_t^2 \\ 0 & -k_{nn}k_{ss}\tau\sigma_n c^2 f_t^2 & k_{nn}k_{ss}\sigma_n^2 c^4 \end{bmatrix}$
Slipping	$[D_{ep}] = \frac{t}{k_{ss} + k_{nn}\gamma}$	$\begin{bmatrix} 0 & 0 & 0 \\ 0 & k_{nn}k_{ss} & k_{nn}k_{ss}\tan\phi \\ 0 & k_{nn}k_{ss}\tan\phi & k_{nn}k_{ss}\gamma \end{bmatrix}$
Crushing	$[D_{ep}] = \frac{t}{k_{ss}\tau_f^2 + k_{nn}\sigma_n^2 c^4}$	$\begin{bmatrix} 0 & 0 & 0 \\ 0 & k_{nn}k_{ss}\tau_f^4 & -k_{nn}k_{ss}\tau\sigma_n c^2 f_c^2 \\ 0 & -k_{nn}k_{ss}\tau\sigma_n c^2 f_c^2 & k_{nn}k_{ss}\sigma_n^2 c^4 \end{bmatrix}$

$\{\Delta\}_{i-1}$ = Accumulated displacement at load increment i-1:

The incremental strains $\{\Delta\varepsilon\}_i$ can be evaluated by using the following relation:

$$\{\Delta\varepsilon\}_i = [B]\{\Delta\delta\}_i \quad (14)$$

The total strain $\{\varepsilon\}_i$ after the i^{th} load increment is then obtained as:

$$\{\varepsilon\}_i = \{\varepsilon\}_{i-1} + \{\Delta\varepsilon\}_i \quad (15)$$

Where $\{\varepsilon\}_{i-1}$ are the strain vectors at the end of (i-1)th load increment. Similarly, the increment of stresses $\{\Delta\sigma\}_i$ are determined as:

$$\{\Delta\sigma\}_i = [D]_{ep}\{\Delta\varepsilon\}_i \quad (16)$$

Where $[D]_{ep}$ is the elasto-plastic material matrix (Nayek, et al [14]), $\{\varepsilon\}_{i-1}$ and stress $\{\sigma\}_{i-1}$ levels calculated at the end of the previous iteration, taking into account the yielding, loading and unloading at the Gauss point under consideration

as in the case of conventional finite elements. The plastic deformation in a thin layer interface is allowed to occur whenever stress exceeds the envelope presented by a modified Mohr-Coulomb failure criteria presented in Figure 2. Based on the theory of plasticity the evolved nonlinear elasto-plastic constitutive models (shown in Table 2) have been implemented in different formulations to represent debonding slipping, and crushing along discontinuities.

The total stresses $\{\sigma\}_i$ are determined as:

$$\{\sigma\}_i = \{\sigma\}_{i-1} + \{\Delta\sigma\}_i \quad (17)$$

Several iterations are needed to bring the stresses to the yield surface in case of yielding occurrence at the Gauss point under consideration.

4. RESIDUAL FORCES

The residual or unbalanced force vector $\{R\}^i$ will be evaluated using the relationship:

$$\{R\}^i = \{F\}^i - \int [B] \{\sigma\}^i dV \quad (18)$$

Where $\{F\}^i$ is the total applied load vector after the application of the i^{th} load increment, while $\{\sigma\}^i$ and $[B]$ are the total stress vectors and the strain-displacement matrix respectively at the i^{th} load increment.

The residual forces will be checked against the chosen convergence criterion. If the convergence criterion is not satisfied, the residual forces are to be applied to the structure as a corrective load and the corresponding corrective displacement increment will be calculated and added to the total displacements.

The process of calculating and applying the residual forces is repeated until the chosen convergence criterion is satisfied.

5. CONVERGENCE CRITERION

The convergence of the numerical process to the nonlinear solution must be defined by comparing, the values of the unknowns ϕ is determined during

each iteration in order to terminate the iterations during a load increment.

The displacement or the force criteria may be used to set the solution tolerance which may be expressed as (Noorzaei, et al [15,16]):

$$\frac{\sqrt{\left[\sum_{i=1}^N (\phi_i^r)^2 \right]} - \sqrt{\left[\sum_{i=1}^N (\phi_i^{r-1})^2 \right]}}{\sqrt{\left[\sum_{i=1}^N (\phi_i^1)^2 \right]}} \times 100 \leq \text{TOLER} \quad (19)$$

Where N is the total number of nodal points in the problem and r-1 and r denotes the successive iterations. The multiplication factor of 100 on the left side allows the specified tolerance factor TOLER to be considered as a percentage term. In practical situations a value of TOLER = 1.0 (i.e 1.0) is found to be adequate for the majority of applications (Viladkar, et al [17]).

5.1. Finite Element Computer Code The existing two dimensional plane stress, plane strain and axi-symmetric finite element code which was developed by Noorzaei, et al [15,16] has been extensively modified in view of the enhancement of the program capabilities for both linear and elasto-plastic analysis under static loading. The finite element code has been further strengthened by incorporating a thin layer element in its element library and also including the constitutive elasto-plastic models of a thin layer interface element. Figure 3 shows the overall schematic flow chart of the finite element code developed in the present investigation. The finite code is a multi-element, multi degrees freedom and multi-yield criterion in nature.

5.2. Validation and Verification of the Developed Finite Element Code In order to check the accuracy of the formulation, implementation and computer codification, several bench mark examples have been analyzed and only two examples are presented herein.

5.2.1. Example

Thin layer interface element under plane strain Figure 4 shows the idealization of a simple plane

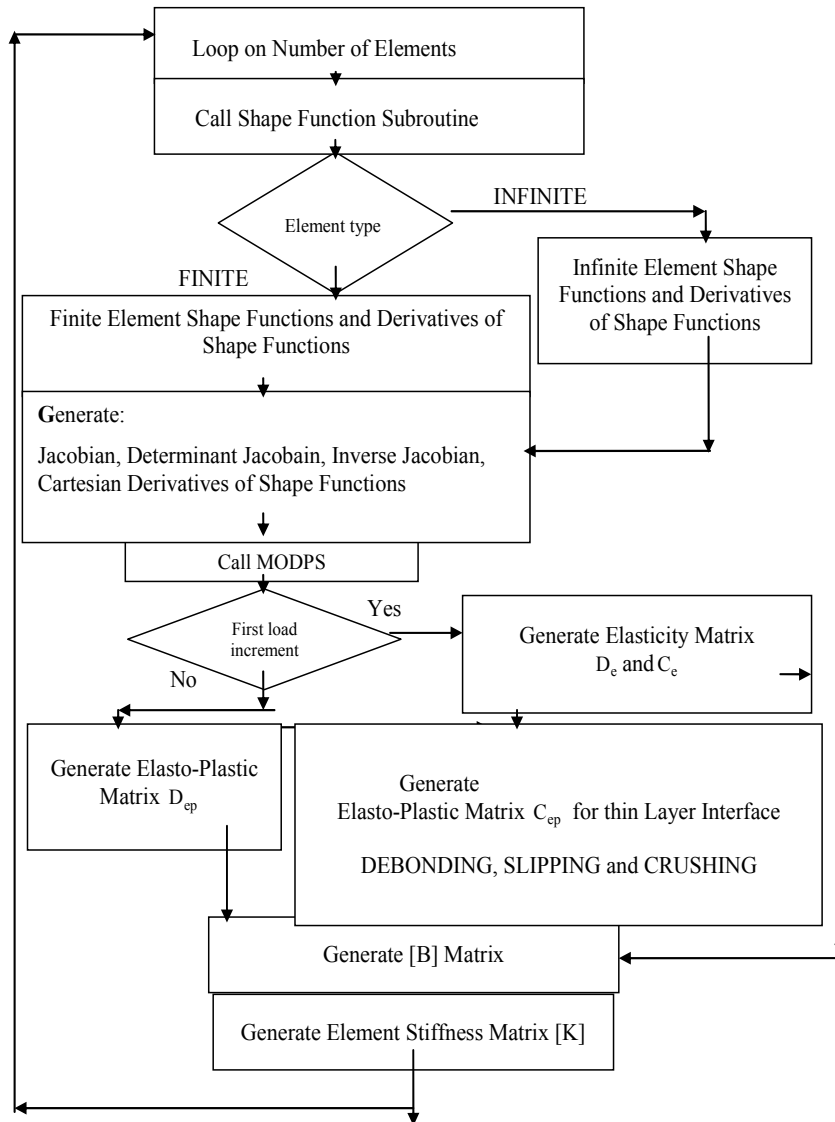


Figure 3. Flowchart of elasto plastic 2-D multi-element algorithm.

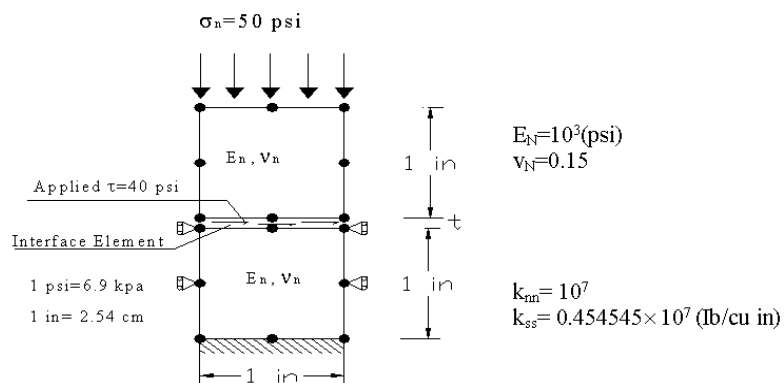


Figure 4. Finite element model.

strain problem with a horizontal thin layer interface element (Sharma, et al [18]) that is subjected to static loading. The analysis was performed using the units presented in the paper for the material properties.

The stress distribution obtained from the present study is compared with those reported by Sharma as tabulated in Table 3. Results corresponding to the average shear stress for various t/B , thin layer interface element are presented in Table 3. It is obvious from this table that the implementation of a thin layer interface in a computer program is capable of accurately tracing the discontinuity along the stress distribution.

5.2.2. Example

Foundation soil-interaction In order to further investigate the response of a thin layer element between two different materials under a plane strain condition, a problem of foundation soil interaction has been selected as shown in Figure 5. The footing is subjected to vertical and lateral loads simultaneously.

The study was carried out using three different finite element models namely:

- (a) Finite element analysis without a thin-layer element (FEWI) with 131 nodes and 34 elements.

TABLE 3. Average Shear Stress (τ).

Exact Value of Shear Stress = 40 psi			
t/B		Average Shear Stress (psi)	% Difference
0.1	Sharma	40.00	-0.012 %
	Present Study	39.995	
0.01	Sharma	40.00	0.0 %
	Present Study	40.00	
0.001	Sharma	40.00	0 %
	Present Study	40.00	

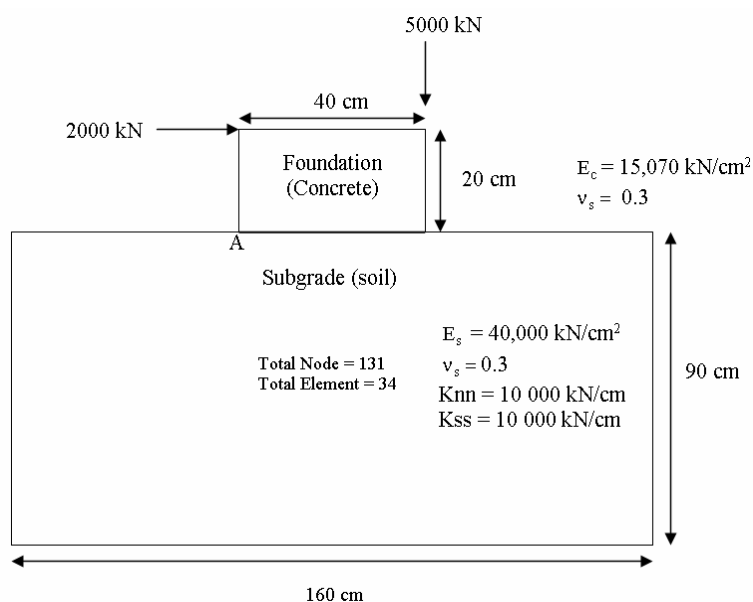


Figure 5. Thin layer interface element.

- (b) Finite element analysis with a six node thin-layer element (FE6Th) with 140 nodes and 38 elements.
- (c) Finite element analysis with an eight node thin-layer element (FE8Th) with 145 nodes and 38 elements.

The comparison between the maximum displacements in the vertical and lateral directions has been made in Table 4. It is seen from this table that all models, result in almost identical results. This indicates that the thin element formulation, computer codification has been carried out correctly.

It is seen from this table that all the idealization yields almost the same results, which indicates that the formulation, computer codification of the thin layer has been carried out correctly.

6. ANALYSIS OF A RAILWAY TRACK BEDDING SYSTEM

6.1. Problem Definition In Malaysia, usually a typical 5-meter high embankment of double tracking projects is adopted. A UIC 54 kg rails (169 mm) are provided over the concrete sleepers, which are placed at 600 mm spacing. The sleepers rest over a 300 mm (minimum) thick ballast layer and 300 mm thick sub-ballast layer. The typical geometry of the railway track bedding system is shown in Figure 6.

The railway track supporting system was idealized under a plane strain condition (Esveld, et al [19]). In fact the sleepers are discrete members and are assumed to be continuous along the length of the track. Besides that, the wheel loads are converted into equivalent loads ($P=57\text{kN}$). Figure 6 shows the finite model for a railway track supporting media through finite- infinite and thin-layer elements. The number and types of elements used in the finite modeling are also summarized in Figure 7.

Due to the fact, that soil is a nonlinear material; the nonlinearity of soil will be taken into consideration, by using the Mohr-Coulomb's Elasto-Plastic model. The material properties adopted for various components of the rail way track system and sub-grade are shown in Table 5.

Based on earlier works published by Desai, et al [20], the material properties for a thin layer element are adapted in present study with

$$K_{nn} = 1000000\text{MPa}, \quad K_{ss} = 1000000\text{MPa},$$

$$\phi = 30^{\circ}, \quad \text{cohesion} = 0.7\text{MPa}.$$

Table 5 shows the lists of different Yielding-Criterion adopted with respect to different types of materials. The mode of load application on a railway track-supporting system was carried out by incremental iterative techniques.

7. RESULTS AND DISCUSSIONS

7.1. Linear Static Response

7.1.1. Displacement Figure 8 shows the variation of the displacement along the depth of the railway supporting system at some specific sections namely, A-A, B-B, C-C and D-D. It is clear from this plot that due to the symmetrical nature of the loading, the displacement variation is highest (14 mm) at the top and lowest (nearly zero) at the bottom.

7.1.2. Stresses The contact pressure distributions for horizontal sections E-E, F-F, G-G and H-H, along the depth of the supporting media are presented in Figure 9. These horizontal sections are located at different depths as indicated in this plot. It is clear from this figure that the maximum σ_y calculated at the top is exactly below the point of load application and its value reduces along the depth of the supporting media. Due to the symmetrical nature of the loading, the trend in variation and distribution of the stresses are influenced by the location of the load application and the stiffness of the supporting media.

A similar response to contact pressure distribution has been reported by Martin, et al [21].

The plots on variation of principal stresses σ_1 and σ_3 are presented in Figures 10 and 11 respectively. These plots are made at different horizontal planes along the depth of the soil-system. It can be seen from these plots that as it was expected the maximum values of both the principal stresses are evaluated at the top of the

TABLE 4. Comparison of the Maximum Deflection in Vertical and Lateral Directions.

Item	Types and Analysis		
	FEWI	FE6Th	FE8Th
Maximum Vertical Displacement (cm)	3.745	3.764	3.734
Maximum Lateral Displacement (cm)	2.291	2.337	2.306

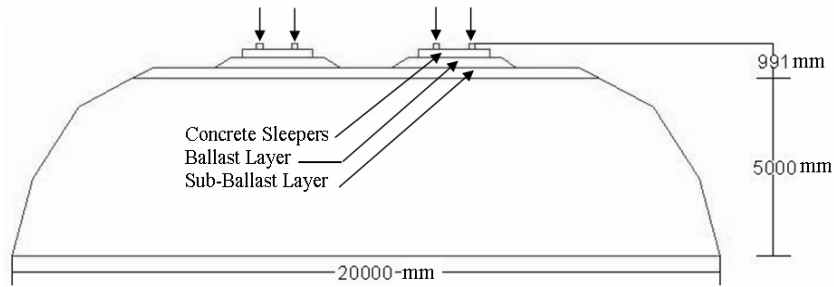


Figure 6. Typical Geometry for railway track-supporting media.

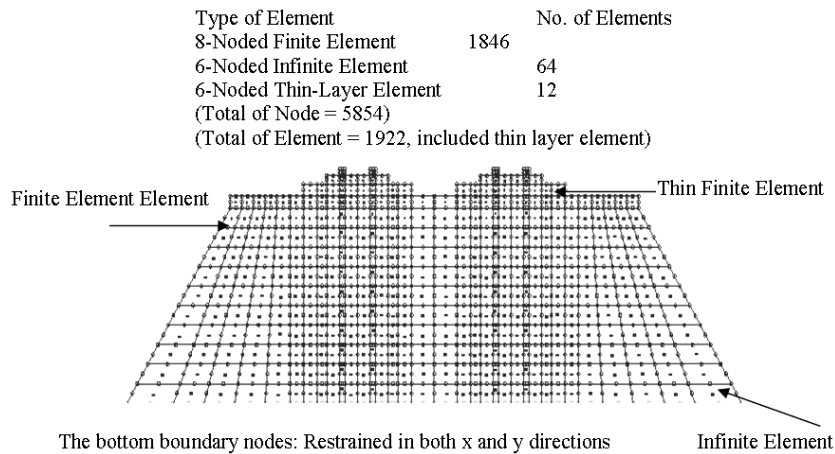


Figure 7. Typical geometry for railway track-supporting media.

TABLE 5. Constitutive Modeling.

Components	Adopted Criteria	Yield Criterion
Rail (Steel)	Von-Mises Method	$f = \tau - \sigma_n \tan \phi$
Sleeper (Concrete), Ballast and Sub-Ballast	Drucker-Prager Method	$f = \alpha J_1 + J_2^{1/2} - K$
Soil Media and Thin-Layer Element (Contact Area Between Sleeper and Ballast)	Mohr-Coulomb Method	$f = \sqrt{3J_2'} - Y(K)$

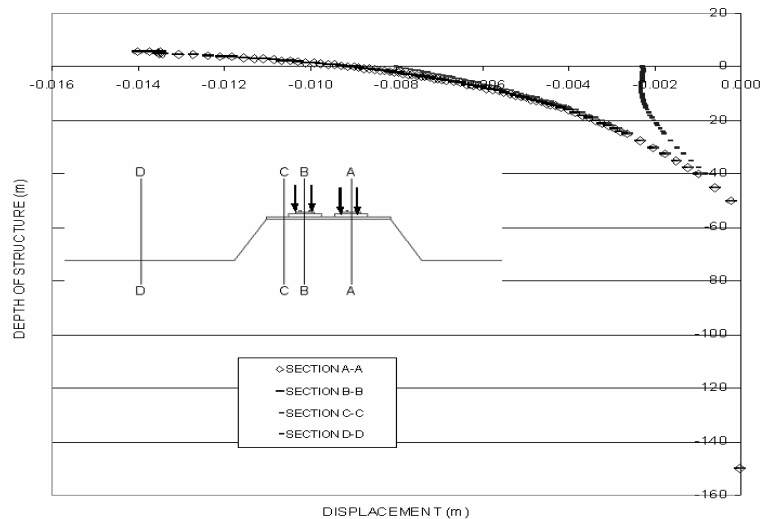


Figure 8. Variation of vertical displacement along depth of track-supporting media.

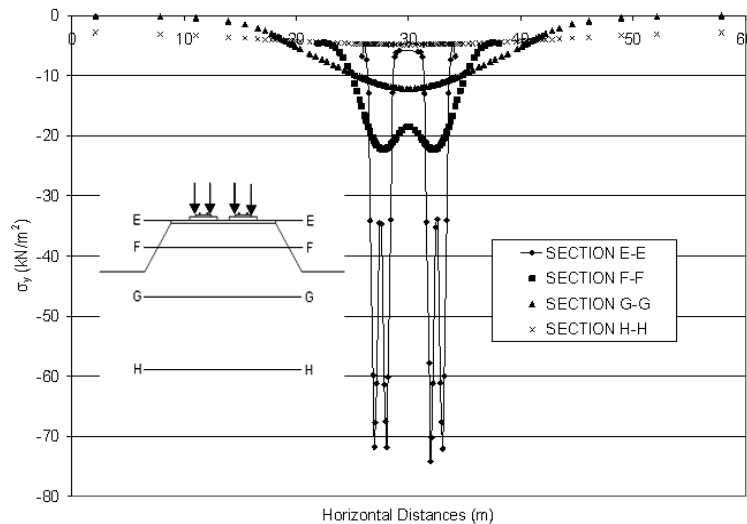


Figure 9. Contact pressure (σ_y) distribution at different horizontal sections.

horizontal layer (section E-E) and exactly below the load zone application. Martin, et al [21] has predicted a similar response.

7.1.3. Elasto-plastic analysis In order to assess the safety of the railway track supporting media, an elasto-plastic finite element analysis was performed. The yield pattern of the railway track supporting media at different load factors, namely 3 (three times the applied load), 5 and 10 are illustrated in Figures 12a-c respectively. A critical study of

yielding patterns indicates that the plastic flow initially started from the rail and sleeper and then flowed vertically downwards and finally moved towards the centre of the railway-line. In the elasto plastic finite element analysis, the collapse is deemed to have occurred if the iterative procedure diverges for a particular load increment (Owen, et al [22], Noorzaei, et al [15], Viladkar, et al [17]). It is evident from these plots at the load factor (LF=10) there is no occurrence of divergence in the elasto-plastic analysis.

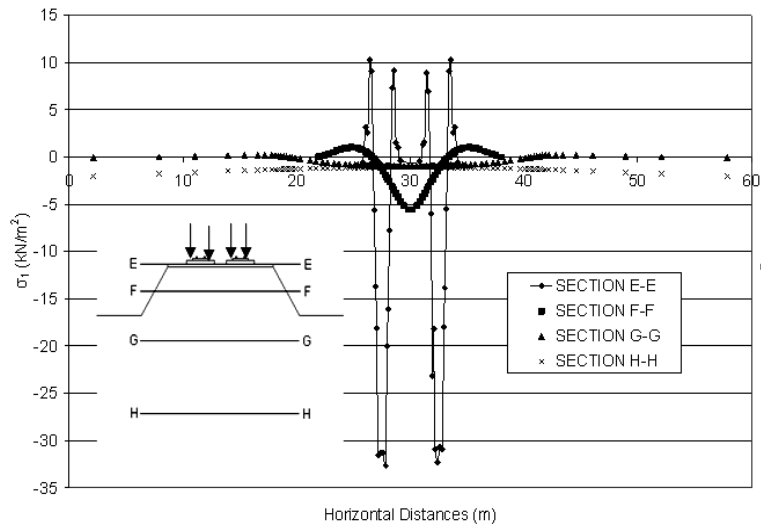


Figure 10. Variation of maximum principle stress (σ_1) at different horizontal sections.

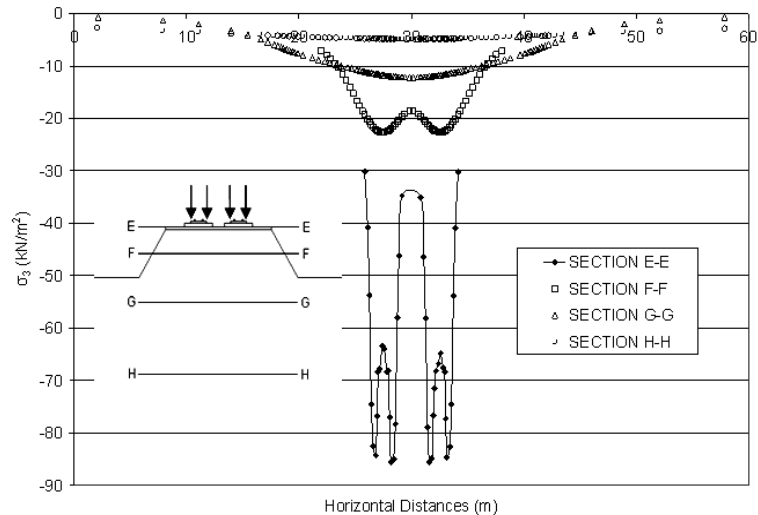


Figure 11. Variation of minimum principle stress (σ_3) at different horizontal sections.

8. CONCLUSIONS

A two dimensional F.E code was developed based on the proposed physical and material constitutive models. The application of the couple finite-infinite and thin layer interface elements in the physical modeling of the railway track supporting system has been demonstrated. Through a multi-yield criterion to represent the materials' nonlinearity for steel, concrete and soil as represented by Von Mises, Drucker-Prager and Mohr coulombs elasto-

plastic constitutive models respectively has been presented. The finite element program has been validated against two examples.

From the numerical results obtained in this work as a case study on an actual railway track supporting media, the following points can be highlighted.

- Due to the symmetrical nature of loading, the displacement variation is highest (14 mm) at the top and lowest (nearly zero) at the bottom.

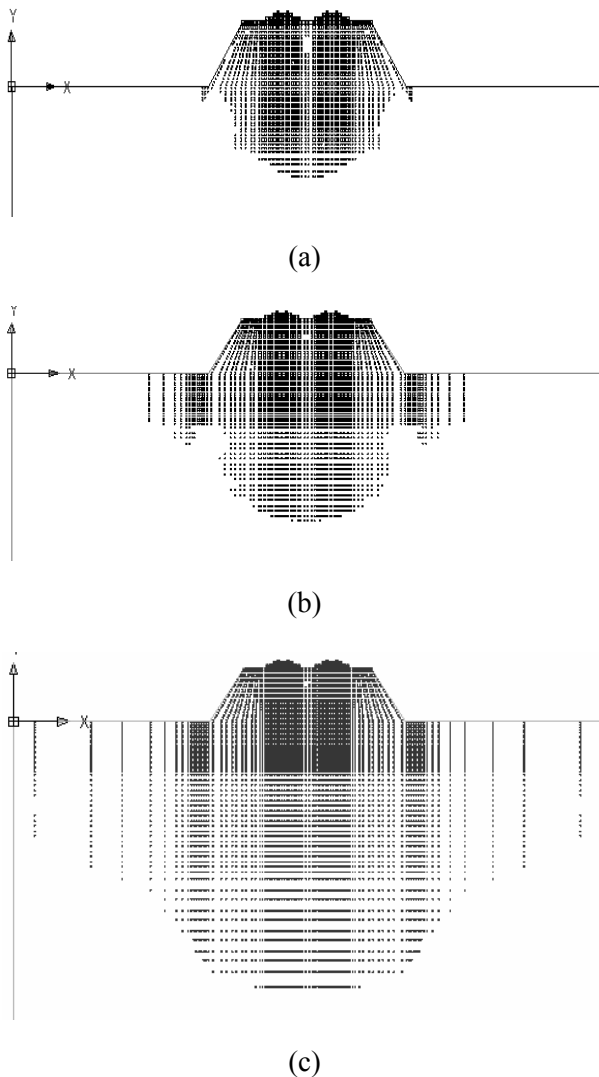


Figure 12. Spread of plastic zone in railway track-sleeper-ballast-sub-ballast-support at different load factors, (a) load factor = 3, (b) load factor = 5 and (c) load factor = 10.

- The maximum normal vertical stress calculated was exactly below the application load point and its value reduces along the depth of the supporting media.
- It was seen that during an incremental-iterative application of external loads, the yielding modes started from the rail and then flowed vertically down to the centre line of the railway track-supporting system. Up to L.F = 10, there was no sign of any plastic flow in the railway track-supporting structure.

9. REFERENCES

1. Desai, C.S., Zaman, M.M. and Siriwardane, H.J., "Numerical Models for Track Supported Structures", *International Journal of the Geotechnical Engineering, ASCE*, Vol. 108, No. GT3, (1982).
2. Desai, C.S., Zaman, M.M. and Muqtadir, A., "3-D Analysis of Some Soil Structure Interaction Problems", Recent Development in Laboratory and Field tests and Analysis of Geotechnical Problems, Bangkok, Thailand, (1983), 551-562.
3. Chang, C.S., Adegoke, C.W. and Selig, E.T., "Geotrack Model for Railroad Track Performance", *Journal of the Geotechnical Engineering, ASCE*, Vol. 106, No. GT11, (1980), 1201-1218.
4. Mauro, C., Anders, E., Alan, F., Giampaolo, M. and Maurizio, S., "Prediction of Rail Vehicle Mission Loads and RCF Damaged by Multibody Modeling", *Proceeding Ist MSC. ADAMS. European User Conference*, London, U.K., (2002).
5. Lombaert, G., Degrande, B., Vanhauwere, B.V. and Francois, S., "The control of Ground-Borne Vibration from Railway Traffic by Means of Continuous Floating Slabs", *Journal of Sound and Vibration*, Vol. 297, No. 6, (2006), 946-961.
6. Michael, J., Steenbergan, M. M. and Andrei, V. M., "The Effect of the Interface Conditions on the Dynamic Response of a Beam on a Half Space to a moving load", *European Journal of Mechanics-A/Solids*, Vol. 26, (January-February 2007), 33-54.
7. Zienkiewicz, O.C., "The Finite Element Method in Engineering and Science McGraw-Hill", 5th edition, New Delhi, India, (1983).
8. Godbole, P.N., Viladkar, M.N. and Noorzaeei, J., "Nonlinear Soil-Structure Interaction Analysis using Coupled Finite-Infinite Elements", *Computers and Structures*, Vol. 36, (1990a), 1089-1096.
9. Viladkar, M.N., Godbole, P.N. and Noorzaeei, J., "Some New Three-Dimensional Infinite Elements", *Computers and Structures*, Vol. 34, (1990b), 455-467.
10. Viladkar, M.N., Godbole, P.N. and Noorzaeei, J., "Soil-Structure Interaction in Plane Frames using Coupled Finite-Infinite Elements", *Computers and Structures*, Vol. 39, (1991), 535-546.
11. Desai, C.S., Drumm, E.C. and Zaman, M.M., "An Interface Model for Dynamic Soil-Structure Interaction", *Journal of Geotechnical Eng. Div., ASCE*, Vol. 110, (1984a), 1257-1273.
12. Desai, C.S., Zaman, M.M., Lightner, J.G. and Siriwardane, H.J., "Thin-Layer Element for Interfaces and Joints", *International Journal for Numerical and Analytical Methods in Geomechanics*, Vol. 8, No. 1, (1984b), 19-43.
13. Linsbauer, H.N. and Bhattacharjee, S., "Dam Safety Assessment due to Uplift Pressure Action in a Dam-Foundation Interface Crack", Fifth Benchmark Workshop on Numerical Analysis of Dams, Denver, Colorado, U.S.A., (1999).
14. Nayak, G.C. and Zienkiewicz, O.C., "Elasto-Plastic Stress Analysis. A Generalization Forvarious Constitutive Relations Including Strain Softening", *Int. J. Numer.*

- Meth. Eng.*, Vol. 5, No. 1, (1972), 113-135.
15. Noorzaei, J., Viladkar, M.N. and Godbole, P.N., "Influence of Strain Hardening on Soil Structure Interaction of Framed Structures", *Computers and Structures*, Vol. 55, (June 3, 1995a), 789-795.
 16. Noorzaei, J., Viladkar, M.N. and Godbole, P.N., "Elasto-Plastic Analysis for Soil-Structure Interaction in Framed Structures", *Computers and Structures*, Vol. 55, (June 3, 1995b), 797-807.
 17. Viladkar, M.N., Noorzaei, J. and Godbole, P.N., "Nonlinear Soil Structure Interaction of Plane Frames", *International Journal of Computers Aided Engineering and Software*, Vol. 11, (1994), 303-316.
 18. Sharma, K.G. and Desai, C.S., "Analysis and Implementation of Thin Layer Element of Interface and Joints", *Journal of Engineering Mechanics, ASCE*, Vol. 118, No. 12, (1992), 545-569.
 19. Esveld, C. and Kok, A.W.M., "Interaction Between Moving Vehicles and Railway Track at High Speed", *Rail Engineering International*, Vol. 27, No. 3, (1998), 14-16.
 20. Desai, C.S., Somasundram, S. and Frantziskonis, G., "A hierarchical Approach for Constitutive Modeling of Geologic Materials", *International Journal for Numerical and Analytical Methods in Geomechanics*, Vol. 10, (1986), 225-257.
 21. Martin, X.D., Torbjornt, L.E. and Wiberg, N.E., "Modeling of Railway Vehicle-Track Underground Dynamic Interaction Induced by High Speed Trains", International Publication, Chalmerse University of Technology Sweden, Göteborg, Sweden, (2003).
 22. Owen, D.R.J. and Hinton, E., "Finite Element in Plasticity: Theory and Practice Pineridge Press Limited", U.K., (1980).